Impact of Modeling Approach on Flutter Predictions for Very Large Wind Turbine Blade Designs

Brian C. Owens
bcowens@sandia.gov
Graduate Student Intern
Wind Energy Technologies Department
Sandia National Laboratories*
Albuquerque, New Mexico, U.S.A.

D. Todd Griffith
dgriffi@sandia.gov
Principal Member of Technical Staff
Wind Energy Technologies Department
Sandia National Laboratories*
Albuquerque, New Mexico, U.S.A.

Brian R. Resor
brresor@sandia.gov
Senior Member of Technical Staff
Wind Energy Technologies Department
Sandia National Laboratories*
Albuquerque, New Mexico, U.S.A.

John E. Hurtado
jehurtado@tamu.edu
Associate Professor
Department of Aerospace Engineering
Texas A&M University
College Station, Texas, U.S.A

ABSTRACT

Recent predictions for very large wind turbine blades have indicated that flutter may be a significant concern. Indeed, previous predictions showed a decreasing flutter margin (ratio of flutter speed to operating speed) with an increase in blade length. Previous flutter predictions were performed with a NASTRAN based flutter prediction tool that was originally developed for vertical-axis wind turbine blades. Recently, a new flutter prediction tool has been developed using a custom finite element framework. This new tool has the capability to provide a better geometric representation of a blade and also provides automated algorithms to perform iterative flutter calculations. In the course of applying the newly developed tool to very large blade designs, potential issues with modeling approaches were identified. The choice of aeroelastic representation for flutter analysis of very large wind turbine blades was reevaluated, and revised flutter analysis under different representations shows different flutter predictions for very large blade designs.

INTRODUCTION

Dynamic aeroelastic instability or "flutter" is a self-starting and potentially destructive vibration where aerodynamic forces on a lifting structure couple with the structure's natural modes, producing large-amplitude, diverging periodic motion. Flutter is a common consideration for aircraft which may be exposed to a variety of operating conditions. Historically, flutter has not been a design issue for utility-scale wind turbine blades. However, previous estimates of flutter speed for a variety of turbines have shown that as blades grow in length, the margin of estimated flutter speed relative to turbine operating speed decreases (Refs. 1,2). Newly developed flutter tools with a better geometric representation of turbine blades predict differing flutter trends than previous tools for very large blade designs. This paper discusses a newly developed aeroelastic stability design tool for turbine blades, takes a critical view of existing modeling approaches, and assesses applicability of these approaches to very large blade designs.

Classical flutter (Refs. 3–5) examines the effects of aerodynamic loads on the dynamic stability of a structure. Vortex shedding at the trailing edge of an oscillating lifting surface results in unsteady aerodynamic effects that depend on the motion of the structure. Examination of unsteady aerodynamic theory developed by Theodorsen (Ref. 3) reveals that unsteady aerodynamic effects may be considered as aerodynamic mass, damping, and stiffness terms and combined with the structural coefficient matrices of a dynamic system. Thus, modal analysis may be employed to assess the stability of an elastic system under aerodynamic effects (aeroelastic system). Aeroelastic analysis of an aircraft may consider stability at particular operating conditions such as airspeed and altitude. A similar analogy exists for a wind turbine blade, with the operating condition being the rotor speed of the hub the turbine blade is affixed to.

*Sandia National Laboratories is a multi-program laboratory managed and operated by Sandia Corporation, a wholly owned subsidiary of Lockheed Martin Corporation, for the U.S. Department of Energy's National Nuclear Security Administration under contract DE-AC04-94AL85000.

Presented at the AHS 69th Annual Forum, Phoenix, Arizona, May 21–23, 2013.

Previous work by Lobitz (Ref. 1) considered the flutter analysis of an isolated wind turbine blade rotating in still air. The turbine blade was considered to be cantilevered at the root, and analysis was performed in a rotating frame. Such a system has been termed a "Gyric" system in the literature (Ref. 6) in that it is a linear representation of a flexible structure under a prescribed angular velocity. Considering the system in the rotating frame allows for rotational effects such as "spin softening" and "Coriolis" effects to be considered in a straightforward manner. Accounting for centrifugal loads on the reference position of the blade allows for "stress stiffening" effects to be accounted for. These effects model the increased stiffness of a structure under load, and may significantly affect the modal response of a flexible system.

Lobitz employed the NASTRAN finite element software (Ref. 7) to account for the majority of structural dynamics calculations. The use of DMAP (Ref. 8) programming allowed the NASTRAN finite element matrices to be modified to include aerodynamic effects in the form of aerodynamic mass, damping, and stiffness. A key characteristic of Theodorsen's unsteady aerodynamic theory is the complex valued "Theodorsen" function which accounts for the amplitude reduction and phase lag in aerodynamic forcing on an oscillating structure as a result of shed vortices. Lobitz employed the use of the complex eigensolver in NASTRAN to ease the DMAP implementation of the complex valued aerodynamic terms. The tool, which was originally developed for considering flutter in vertical-axis wind turbines was applied to utility scale horizontal-axis wind turbine blades. This tool was used to investigate the ramifications of using simplified aerodynamic theory (quasi-steady) in flutter analysis of wind turbine blades. The analysis tool was also employed to investigate the effects of flap-twist coupling on the flutter of turbine blade designs.

Hansen (Ref. 9) also considered flutter of wind turbines, but considers stall induced vibration. This is a fundamentally different phenomenon from classical flutter. It should be noted that classical flutter tends to be more catastrophic in nature than stall induced vibrations. Furthermore, classical flutter is typically a concern for pitch regulated turbines while stall-induced vibrations tend to be a concern in stall regulated turbines. Hansen considered modeling of a complete turbine (tower and rotor) and the aeroelastic interaction of stall induced vibrations with the inflow/wake.

This work examines the problem of classical flutter for an isolated wind turbine blade rotating in still air. A newly developed aeroelastic stability tool for horizontal axis wind turbine blades is discussed in this paper. Features and enhancements relative to the legacy flutter tool by Lobitz are highlighted. Flutter analysis of two blade configurations is presented, and potential limitations of the current modeling approach applied to very large wind turbine blades are discussed. Various aeroelastic representations are considered and ramifications of certain modeling approaches are realized. Finally, necessary future work for modeling aeroelastic instabilities in very large wind turbine blades is highlighted.

BLADE AEROELASTIC STABILITY TOOL

The Sandia National Laboratories (SNL) BLade Aeroelastic Stability Tool (BLAST) is a finite element design tool capable of predicting aeroelastic stability characteristics of wind turbine blades with arbitrary geometry and material composition. This tool is an extension of the legacy SNL NASTRAN based flutter tool (Ref. 1), but is developed within a custom finite element framework. This allows complete authority of code development and analysis capabilities. BLAST is programmed in MATLAB, which allows the software to be extremely portable and integrated with the SNL blade design tool NuMAD (Ref. 10).

As with the legacy flutter tool, the underlying formulation of this analysis tool accounts for gyroscopic effects (spin softening and Coriolis), which introduce couplings into the fundamental motions of a blade. Due to the slender nature of turbine blades, beam theory is employed to represent the deformation of the blade. This is believed to be adequate for initial design studies such as flutter analysis. The formulation also accounts for couplings that arise from composite material layups, provided that coupling factors are calculated from a pre-processor for obtaining effective section properties of a blade design (BPE (Ref. 11), PreComp (Ref. 12), VABS (Ref. 13), etc.).

Formulation

The inertial velocity of a point in a rotating hub frame is considered using transport theorem (Ref. 14).

$$\vec{v} = \frac{d}{dt}^{(N)}(\vec{r}) = \left(\vec{\Omega}_{H/N} \times \vec{r}\right) + \frac{d}{dt}^{(H)}(\vec{r}) \tag{1}$$

Such that $\vec{\Omega}_{H/N}$ is the angular velocity vector of the hub frame with respect to the inertial frame (the angular velocity vector of the turbine rotor) and $\vec{r}$ is some arbitrary point in the hub frame. The superscripts N and H denote derivatives with respect to the inertial and hub frame respectively. Although the details are omitted from this paper, this general expression for velocity in a rotating frame, along with the constitutive relations of Euler-Bernoulli beam theory are employed in conjunction with Hamilton's extended principle shown below to arrive at differential equations of motion for a dynamic beam in a rotating frame.

$$\delta \int_V (\mathscr{T}(q,\dot{q}) - \mathscr{V}(q))\, dV = \delta \mathscr{W}_{np} \tag{2}$$

Such that $\mathscr{T}(q,\dot{q})$ is the kinetic energy of a point in the beam accounting for local displacements and rigid body rotation. Here, q and $\dot{q}$ are generalized displacements and velocities respectively. The function $\mathscr{V}(q)$ is a potential energy function composed of the strain energy as governed by Euler-Bernoulli beam theory. $\mathscr{W}_{np}$ represents the work of non-potential forces that cannot be represented in the potential energy function. The variational operator is denoted by δ. This will be used to introduce aerodynamic effects into the formulation. Using Hamilton's principle, the governing equations of motion for a

beam in a rotating frame can be formulated. Introduction of the weak form and Galerkin approximation (Ref. 15) allow for a finite element formulation to be constructed. The finite element formulation allows for a number of beam elements to be employed to construct a turbine blade of arbitrary geometry.

For a parked blade, the resulting system of equations for a finite element representation takes the familiar second order form:

$$M\ddot{q} + C\dot{q} + K(q)q = F_{np} \tag{3}$$

Such that M, C, and K are structural mass, damping, and stiffness matrices respectively. Note the possible geometric nonlinearity in the structural stiffness matrix. F_{np} denotes a non-potential force vector. Overdots represent explicit time derivatives.

Rotational effects for a constant rotor speed introduce the skew-symmetric Coriolis matrix $G(\Omega)$,the symmetric positive definite spin softening matrix $S(\Omega)$, and the centrifugal loading vector $F_{cent}(\Omega)$. This modifies the second order system of equations as shown below

$$M\ddot{q} + (C + G(\Omega))\dot{q} + (K(q) - S(\Omega))q = F_{cent}(\Omega) + F_{np} \tag{4}$$

Considering Theodorsen's unsteady airfoil theory allows aerodynamic effects to be introduced via the non-potential work function in Hamilton's principle. The expressions for aerodynamic lift and moments are in terms of flapping and twisting motion of a cross-section as shown below.

$$\begin{aligned} L &= \pi\rho b^2\left[\ddot{w} + V\dot{\theta} - ba\ddot{\theta}\right] \\ &+ 2\pi\rho V b C(k)\left[\dot{w} + V\theta + b\left(\frac{1}{2} - a\right)\right] \end{aligned} \tag{5}$$

$$\begin{aligned} M &= \pi\rho b^2\left[ba\ddot{w} - Vb\left(\frac{1}{2} - a\right)\dot{\theta} - b^2\left(\frac{1}{8} + a^2\right)\ddot{\theta}\right] \\ &+ 2\pi\rho V b^2\left(a + \frac{1}{2}\right)C(k)\left[\dot{w} + V\theta + b\left(\frac{1}{2} - a\right)\right] \end{aligned} \tag{6}$$

Here, b is the semi-chord of an airfoil section, a is the location of the elastic axis in semi chord fractions aft of the half chord, U_∞ is the freestream velocity over the blade section, ρ is air density, and $C(k)$ is the complex valued Theodorsen function. The flapwise motion of the blade section is represented by $w(t)$ and the torsional motion of the section is represented by $\theta(t)$.

Here, $k = \frac{\omega b}{U_\infty}$ is a "reduced frequency" dependent on the oscillatory motion of the cross-section. The Theodorsen function $C(k)$ is complex in nature and models the amplitude reduction and phase lag in aerodynamic forcing as a result of unsteady effects due to shed vortices at the trailing edge of a blade section. While expressions for lift are traditionally expressed in terms of freestream velocity U_∞, for a rotating turbine blade $U_\infty = r\Omega$ such that r is the spanwise distance along the blade from the hub axis. Thus, the aerodynamic loads are function of generalized displacements, velocities, and accelerations as well as frequency ω. Aerodynamic mass, damping, and stiffness matrices can be formulated in a finite element formulation, and the aeroelastic second order system with rotational effects is shown below

$$\begin{aligned} &[M + M_A(\Omega)]\ddot{q} + [C + G(\Omega) + C_A(\Omega,\omega)]\dot{q} + \\ &[K(q) - S(\Omega) + K_A(\Omega,\omega)]q = F_{cent}(\Omega) + F_A(\Omega) \end{aligned} \tag{7}$$

Such that $M_A(\Omega), C_A(\Omega,\omega), K_A(\Omega,\omega)$ are aerodynamic mass, damping, and stiffness matrices respectively. The vector $F_A(\Omega)$ represents aerodynamic forces due to nonelastic effects (ie. rigid angle of attack, manufactured blade twist, etc). This concludes the formulation overview for a finite beam element with rotational effects under aerodynamic loading consistent with Theodorsen's unsteady aerodynamic theory. Theodoresen's unsteady theory is formulated in the frequency domain making the above system ideal for modal analysis to assess the aeroelastic stability of the system. For modal analysis, the system of interest is

$$\begin{aligned} &[M + M_A(\Omega)]\ddot{q} + [C + G(\Omega) + C_A(\Omega,\omega)]\dot{q} + \\ &[K(q) - S(\Omega) + K_A(\Omega,\omega)]q = 0 \end{aligned} \tag{8}$$

Analysis procedures

Inspection of Eq. 8 shows the coefficient matrices of the second order system are dependent on rotor speed Ω, system frequency ω, and generalized displacements q. Rotor speed may be specified as an operating condition similar to velocity in a traditional flutter analysis for an aircraft. Furthermore, the equations of motion may be linearized about the equilibrium configuration corresponding to the specified rotor speed. This equilibrium configuration is determined by solving the nonlinear static elasticity equation of motion shown below.

$$[K(q) - S(\Omega)]q = F_{cent}(\Omega) \tag{9}$$

With the equilibrium configuration q_{eq} determined, a linearized system may be analyzed through pre-stressed modal analysis.

$$\begin{aligned} &[M + M_A(\Omega)]\ddot{q} + [C + G(\Omega) + C_A(\Omega,\omega)]\dot{q} + \\ &[K(q_{eq}) - S(\Omega) + K_A(\Omega,\omega)]q = 0 \end{aligned} \tag{10}$$

Unfortunately, the linearized equations of motion are still a function of ω which will be unknown until modal analysis is performed. Thus, an iterative procedure termed "p-k iteration" in the literature (Ref. 4) is employed to converge between a "guess" frequency, and a "predicted" frequency for the system under aeroelastic effects.

The following steps outline the procedure for a flutter analysis as implemented into BLAST:

1. Select a rotor speed (Ω) of interest.
2. Perform a static nonlinear analysis under centrifugal loads at rotor speed Ω to obtain an equilibrium solution.
3. Provide a guess frequency and predict the modal response of the system.

4. Select a mode of interest and update the guess frequency used in the previous step.

5. Repeat steps 3 and 4 until the guess and predicted frequencies for the mode of interest are converged.

6. Select the next mode of interest and repeat steps 3 and 4 until all modes of interest have been explored for the rotor speed specified in step 2.

7. Repeat steps 1 through 6 for all rotor speeds of interest.

8. Examine frequency and damping trends for the system across rotor speeds for potential aeroelastic instabilities.

Post-processing and visualization

To aid the analyst in assessing the aerodynamic stability of blade designs BLAST constructs frequency and damping versus rotor speed curves, and seeks to locate the rotor speed at which a mode exhibits a change from positive to negative damping, indicating the onset of flutter. An example of these plots is shown in Figure 1. BLAST also visualizes mode shapes by plotting the fundamental deformations of the blade flexural axis as shown in Figure 2. BLAST also enables the visualization of mode shapes of a blade as an animation of a three-dimensional blade wire mesh. This animation is constructed by projecting the deformation of the flexural axis to the three-dimensional structure in a manner consistent with beam theory. A snapshot of a mode shape animation is shown in Figure 3.

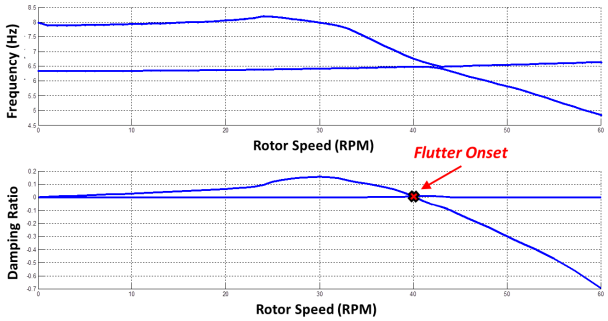

Fig. 1. Frequency and damping ratio vs. rotor speed prediction for a HAWT blade analyzed with BLAST

Enhancements of BLAST relative to the legacy SNL flutter tool

The BLAST analysis tool was developed as an enhanced version of the SNL legacy flutter tool developed by Lobitz (Ref. 1), and the formulation and implementation of BLAST provide a more detailed geometric representation of a blade. This includes better modeling of the flexural axis, as well as sweep and cone of a blade configuration. The legacy flutter tool made use of averaged blade sectional aerodynamic properties while BLAST treats each blade section independently and allows for tapered cross-sectional properties. The effect

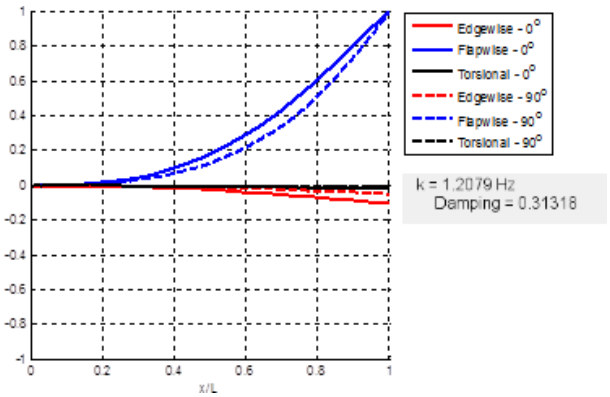

Fig. 2. Example of flexural axis mode shape generated using BLAST

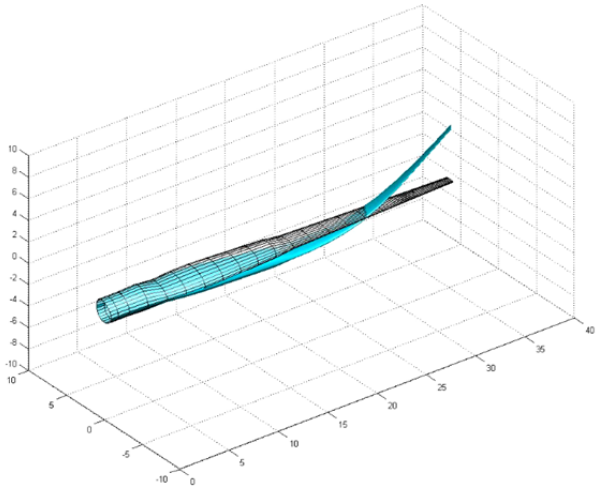

Fig. 3. Snapshot of three-dimensional mode shape animation for HAWT blade

of an offset mass center is considered directly in the underlying formulation of BLAST while the NASTRAN based legacy flutter tool handled offset mass axes in an *ad hoc* manner using concentrated mass and rigid bars attached to a beam flexural axis to model mass and inertia properties of a cross-section.

In addition to differences in the formulation and geometric representation, a key improvement in the BLAST flutter tool is the custom "in-house" framework that eliminates the need for NASTRAN licensing and makes the code widely available to the wind energy community by being packaged with the NuMAD blade design software. This custom framework allows for a leaner, more straightforward implementation that is flexible and expandable for future design tool needs. Flutter analysis using the legacy flutter tool was plagued by the amount of user interaction required to complete a flutter analysis. The iterative procedure described in the previous section was a laborious process when used with the legacy flutter tool. At times, it was difficult to identify a potential flutter mode, and the laborious nature of the analysis procedure prohibited examining a number of modes for the system in a timely manner.

The efficient BLAST software removes the analyst from

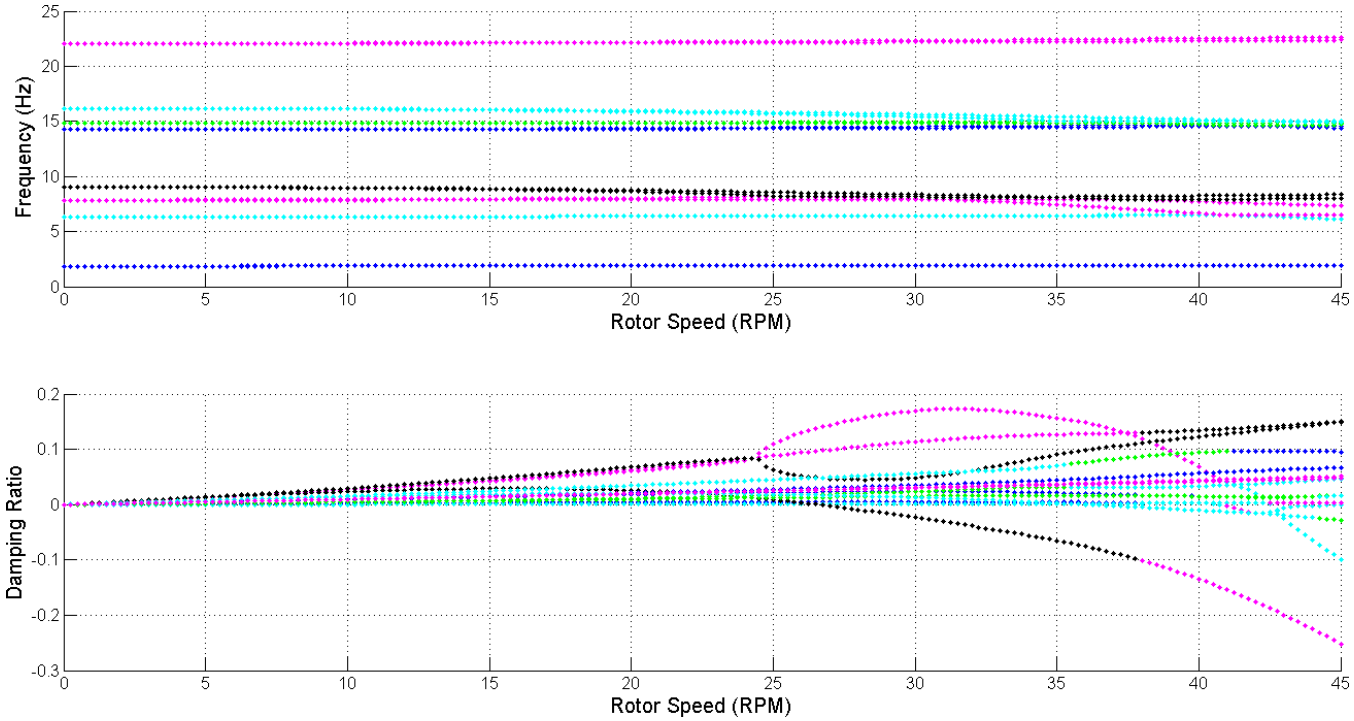

Fig. 4. Frequency and damping ratio vs. rotor speed BLAST predictions for WindPACT 1.5MW blade

the laborious iteration process and performs iteration using an automated algorithm. The analyst simply provides the blade configuration (possibly from the NuMAD blade design tool) and a range of rotor speeds across which to examine aeroelastic stability. Flutter analysis is typically completed in a matter of minutes and frequency and damping curves similar to those shown in Figure 1 are generated for inspection by the analyst. A subset of n lower system modes specified by the user are calculated across the specified rotor speeds using the automated algorithm. Thus, the analyst can devote efforts to interpreting aeroelastic stability trends instead of merely creating them. In addition to flutter of a rotating blade, BLAST also allows for flutter analysis of a parked blade exposed to uniform wind speed and static aeroelastic (divergence) analysis. These analysis capabilities, however, will not be discussed in this paper.

DEMONSTRATION

BLAST was used to investigate two different blade configurations. The first blade considered was a 33 meter "utility scale" blade designed for used on a 1.5MW turbine. The second was a very large 100 meter turbine design. These blades allow one to consider a conventional blade and the current trend of increasing length and flexibility in modern turbine blade designs. The flutter speed of each blade is predicted using BLAST, and potential limitations in the modeling approach are assessed.

The NREL WindPACT 1.5MW blade

The 33 meter NREL WindPACT 1.5MW blade (Ref. 16) has been analyzed using BLAST as well as the legacy flutter tool. This blade has a designed maximum rotor speed of 20.5 RPM. Lobitz predicted a flutter speed of 43.4 RPM (Ref. 1) using the legacy flutter tool. In a comparative effort, BLAST was employed to conduct on a flutter analysis of the WindPACT 1.5MW blade.

The automated nature of BLAST allowed a larger number of lower system modes to be considered over a range of rotor speeds. Figure 4 shows the frequency and damping ratios of a number of modes from 0 to 45 RPM rotor speed using BLAST, and interesting behavior is observed for a number of modes. Interestingly, complex conjugate pairs are not present in the eigenvalues of the system, and this will be discussed in a subsequent section. The analysis revealed potential instabilities (negative damping) onsetting at rotor speeds of 26.6, 36.1, and 42.3 RPM. The 26.6 and 36.1 RPM potential flutter speeds have a "soft" flutter trend or relatively shallow cross over to negative damping at the predicted flutter speed indicating structural damping will likely delay the onset of flutter for these modes. Furthermore, these "softer" modes are typically higher modes of the system. Nevertheless, "hard" flutter or a steep crossover to negative damping is observed for the 42.3 RPM flutter modes. The 42.3 RPM rotor speed is within 2.5% of that predicted by Lobitz. Thus, good agreement is seen considering differences in modeling approaches between the two analysis tools.

Figure 5 shows the mode shape associated with the predicted flutter mode at 42.3 RPM. Analysis of the aeroelas-

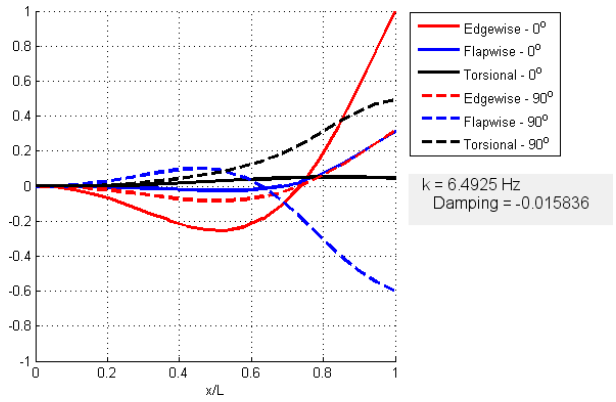

Fig. 5. Flutter mode shape for the WindPACT 1.5MW blade predicted using BLAST

tic system using a state space representation yields complex valued mode shapes. Mode shapes are visualized by examining the real component (0 degree phase mode shape) and the imaginary component (90 degree phase mode shape). The mode shape consists of a first torsional component, 2nd flapwise component, and 2nd edgewise component. The torsional and flapwise modes are characteristic of flutter. The second edgewise component results from the coupling of the flutter mode with an edgewise mode, but can also be attributed to structural twist and couplings arising from the Coriolis rotational effects.

The SNL100-00 blade

The Sandia 100 meter all glass turbine blade (Ref. 17) was also analyzed for flutter instabilities using BLAST. Initial predictions using the legacy flutter tool predicted a relatively low flutter margin on this very large blade (Ref. 2). This blade has been designed with an operational rotor speed of 7.44 RPM.

The BLAST predictions for frequency and damping vs. rotor speed for the SNL100-00 blade are shown in Figure 6. Two potential flutter modes are identified, one at 9.68 RPM (flutter margin of 1.30) and the other 14.40 RPM (flutter margin of 1.94). Neither of these are consistent with previous predictions using the legacy flutter tool for the SNL100-00 (Ref. 2) which predicted a flutter margin around unity for the SNL100-00. This may be due to the differences in geometric representation becoming more significant for the larger SNL100-00 blade than the smaller WindPACT 1.5MW blade analyzed earlier. The lower 9.68 RPM margin of flutter condition exhibits a softer flutter trend and is a higher mode than that of the 14.40 RPM flutter speed mode. Inspection of the mode shapes associated with each of these potential flutter modes shows a 2nd flapwise component coupled with a 1st torsional component which is representative of a classical flutter mode. Under the current modeling approach, BLAST predictions for the SNL100 indicate flutter may not be as significant a concern for larger blades as the legacy flutter tool suggested. Thus, future work should seek to assess the accuracy of aeroelastic predictions of current design tools to predict flutter in very large turbine blade designs.

Furthermore, analysis of this blade reveals trends that are potentially more troublesome than disparities in the predicted flutter speed between the legacy and BLAST software. Typical modal analysis of damped, second order systems through a state space representation results in complex conjugate pair eigenvalues. Essentially, both eigenvalues contain the same frequency and damping information and only half the eigenvalues need to be considered. For the case of the aeroelastic representation in BLAST(as well as the legacy flutter tool) complex conjugate pairs are not present in the eigenvalues of the system. Furthermore, two eigenvalues with comparable frequencies can have drastically different damping trends. Thus, one is surely not justified in only considering half the eigenvalues of the system. The next section seeks to address this concern by obtaining a better understanding of the eigenvalues of systems with complex representations.

CHOICE OF AEROELASTIC REPRESENTATION

As noted in an earlier section, BLAST and the legacy flutter tool both employ a complex valued aeroelastic representation that results in complex valued coefficient matrices for the second order structural dynamics system. In particular, both aerodynamic damping and stiffness matrices are non-symmetric and complex in nature. The resulting system may be analyzed using a complex eigensolver to obtain eigenvalues and eigenvectors related to the stability of the aeroelastic system. Employing a state-space representation to analyze the stability of a conventional damped second order system results in complex conjugate pairs.

The aeroelastic systems for HAWT blades considered in this paper result in a number of modes as shown in Figure 4 and 6 complex conjugate eigenvalue pairs do not exist for this system. Although, it is believed that this was due to the complex nature of the aeroelastic system there were also many other factors at hand including rotational effects and non-ideal geometry. Thus, a simple single degree of freedom problem is considered to show in general modal analysis of a complex valued representation will not result in complex conjugate eigenvalue pairs. Furthermore, this brings into question the physical meaning of eigenvalues of a second order system with complex representation.

An example system with a complex representation

Consider the second order system

$$M\ddot{x} + C\dot{x} + Kx = 0 \tag{11}$$

Here, M is a symmetric, real valued mass matrix. The matrices C and K are damping and stiffness matrices respectively. These matrices may be unsymmetric and may have a complex representation. For example, unsteady Theodorsen dynamics will give rise to unsymmetric, complex representations in the form of aerodynamic damping and stiffness matrices.

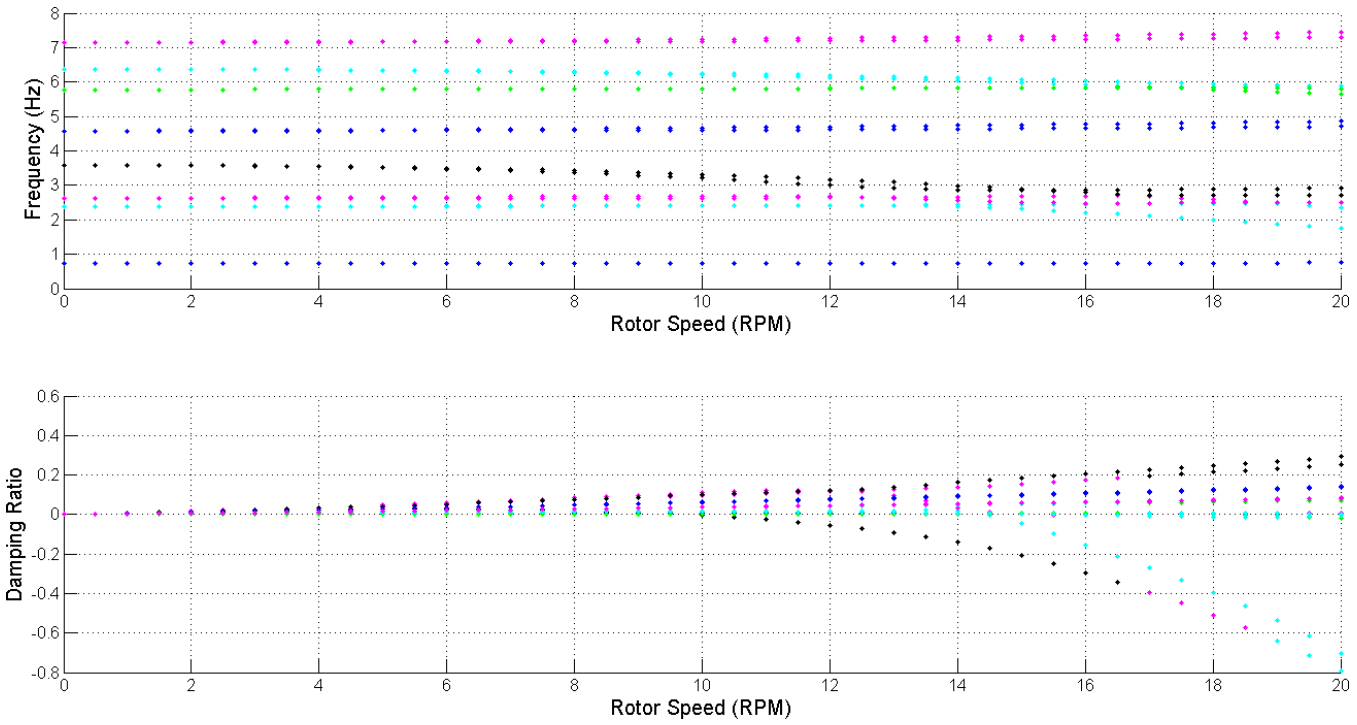

Fig. 6. Frequency and damping ratio vs. rotor speed BLAST predictions for SNL100-00 blade

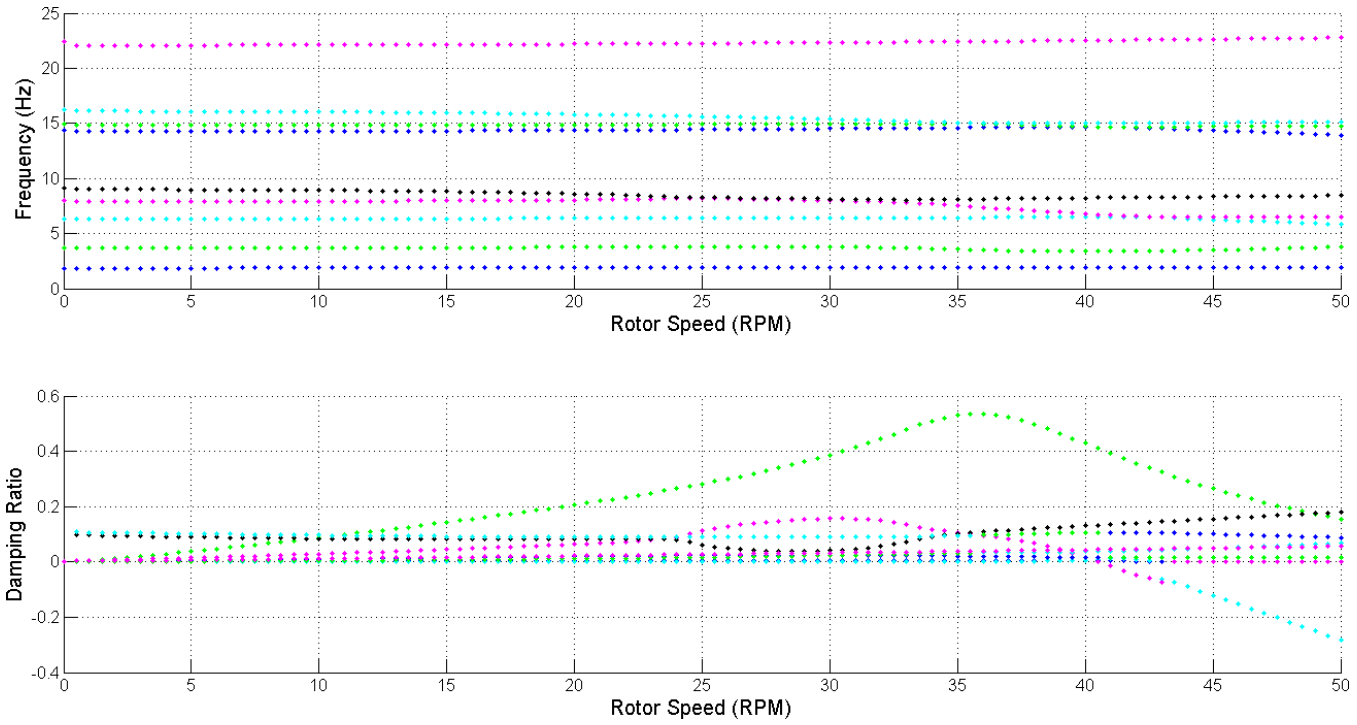

Fig. 7. Frequency and damping ratio vs. rotor speed real valued BLAST predictions for WindPACT 1.5MW blade

Consider the diagonalization of M via a modal matrix, Φ. The modal matrix is composed of eigenvectors that are orthogonal with respect to the mass matrix. Thus, the diagonalized mass matrix, Λ is

$$\Lambda = \Phi^T M \Phi \tag{12}$$

Introducing the following relation

$$x = \Phi \eta \tag{13}$$

and premultiplying the governing equation by Φ^T results in the following system

$$\Phi^T M \Phi \, \ddot{\eta} + \Phi^T C \Phi \, \dot{\eta} + \Phi^T K \Phi \, \eta = 0 \tag{14}$$

$$\Lambda \ddot{\eta} + \Phi^T C \Phi \, \dot{\eta} + \Phi^T K \Phi \, \eta = 0 \tag{15}$$

Now, let a simplifying assumption be made that the off-diagonal elements of the transformed damping and stiffness matrices are small relative to diagonal components

$$\Phi^T C \Phi \approx \hat{C} \tag{16}$$

$$\Phi^T K \Phi \approx \hat{K} \tag{17}$$

Here, $\hat{C}$ and $\hat{K}$ are diagonal, complex matrices. Under these approximations, the system is

$$\Lambda \ddot{\eta} + \hat{C} \dot{\eta} + \hat{K} \eta = 0 \tag{18}$$

The resulting system is decoupled, resulting in multiple single degree of freedom scalar equations

$$\Lambda_j \ddot{\eta}_j + \hat{C}_j \dot{\eta}_j + \hat{K}_j \eta_j = 0 \tag{19}$$

Herein, let the index be dropped and a single degree of freedom scalar equation be considered. The complex representation of the damping and stiffness matrices can be emphasized in this equation as

$$\Lambda \ddot{\eta} + (c + i\,\tilde{c})\,\dot{\eta} + \left(k + i\,\tilde{k}\right)\eta = 0 \tag{20}$$

Suppose the following form of η is assumed

$$\eta = a \exp(\lambda t) \tag{21}$$

$$\dot{\eta} = a\lambda \exp(\lambda t) = \lambda \eta \tag{22}$$

$$\ddot{\eta} = a\lambda^2 \exp(\lambda t) = \lambda^2 \eta \tag{23}$$

Thus, the scalar equations of the decoupled system may be expressed as

$$\left\{\Lambda\lambda^2 + (c + i\,\tilde{c})\,\lambda + \left(k + i\,\tilde{k}\right)\right\}\eta = 0 \tag{24}$$

Solving for λ results in

$$\lambda = -\frac{\hat{C}}{2\Lambda} \pm \frac{1}{2}\sqrt{\frac{\hat{C}^2}{\Lambda^2} - 4\frac{\hat{K}}{\Lambda}} \tag{25}$$

$$\lambda = -\frac{c + i\,\tilde{c}}{2\Lambda} \pm \sqrt{\frac{(c^2 - \tilde{c}^2)}{4\Lambda^2} + i\frac{c\tilde{c}}{2\Lambda^2} - \frac{\left(k + \tilde{k}\right)}{\Lambda}} \tag{26}$$

Let the following expressions be introduced

$$A = \frac{\left(c^2 - \tilde{c}^2\right)}{4\Lambda^2} - \frac{k}{\Lambda} \tag{27}$$

$$B = \frac{c\tilde{c}}{2\Lambda^2} - \frac{\tilde{k}}{\Lambda} \tag{28}$$

Furthermore, let

$$\sqrt{A + iB} = a + i\,b \tag{29}$$

Therefore,

$$\lambda = \left(-\frac{c}{2\Lambda} \pm a\right) + i\,\left(-\frac{\tilde{c}}{2\Lambda} \pm b\right) \tag{30}$$

or

$$\lambda_1 = \left(-\frac{c}{2\Lambda} + a\right) + i\,\left(-\frac{\tilde{c}}{2\Lambda} + b\right) = \lambda_{R_1} + i\,\lambda_{I_1} \tag{31}$$

$$\lambda_2 = \left(-\frac{c}{2\Lambda_j} - a\right) + i\,\left(-\frac{\tilde{c}}{2\Lambda} - b\right) = \lambda_{R_2} + i\,\lambda_{I_2} \tag{32}$$

Note that $\lambda_{R_1} \neq \lambda_{R_2}$ and $\lambda_{I_1} \neq -\lambda_{I_2}$. Thus, in general for a complex representation complex conjugate eigenvalue pairs will not exist. Even for the specific case of no damping ($c = \tilde{c} = 0$) one may observe that

$$\lambda_1 = -\lambda_2 = a + i\,b \tag{33}$$

Identifying Frequency and Damping Information from Eigenvalues

For a real valued, damped system the governing differential equation is often expressed as

$$\ddot{x} + 2\xi\,\omega_n \dot{x} + \omega_n^2 x = 0 \tag{34}$$

Such that ω_n and ξ are the natural frequency and damping ratio of the system respectively. Assuming $x = x_0 \exp(\lambda t)$ allows the eigenvalues to be calculated

$$\lambda_{1,2} = -\xi\,\omega_n \pm i\,\omega_n\sqrt{1 - \xi^2} \tag{35}$$

Inspecting this equation reveals that the eigenvalues of the real valued, damped system will occur in complex conjugate pairs. Indeed, inspection of the system presented in the previous section shows that the eigenvalues of the real valued system (setting $\tilde{c} = \tilde{k} = 0$) are complex conjugate pairs.

For the case of complex systems, it has been shown that in general, complex conjugate pair eigenvalues do not exist. Therefore, extraction of frequency and damping information via the above expression is questionable for systems with complex representations. It is notable that it has been verified that the legacy NASTRAN based flutter tool makes use of a "canned" frequency and damping extraction routine that is only valid for real valued representations. However, the same routine appears to be used for complex valued systems which brings into question the meaningfulness of the frequency and damping values obtained using the NASTRAN flutter tool. Furthermore, the same issue arises in the existing BLAST implementation with respect to the methods for extracting frequency and damping information from the eigenvalues of a complex valued system.

An alternative real valued aeroelastic representation

The previous aeroelastic representation employed in the legacy and BLAST flutter tools did not consider the form of the complex valued Theodorsen function $C(k)$. This complex function was simply calculated and employed in a finite element function as a complex valued constant. One may, however, realize this function in terms of real and imaginary valued functions such that

$$C(k) = F(k) + iG(k) \tag{36}$$

Thus, this form can be employed in the expression of non-potential work in Hamilton's principle and imaginary values can be "absorbed" in the quasi-velocity terms that result from assumed oscillatory motion. That is

$$x = x_0 e^{i\omega t} \tag{37}$$

$$\dot{x} = i\omega x_0 e^{i\omega t} \tag{38}$$

$$\ddot{x} = -\omega^2 x_0 e^{i\omega t} \tag{39}$$

For example, consider the circulatory (due to aerodynamic effects) lift force related to the pitch of the blade section.

$$L_{circ}(\theta, \dot{\theta}) = 2\pi\rho U_\infty b C(k) \left[U_\infty \theta + b\left(\frac{1}{2} - a\right)\dot{\theta} \right] \tag{40}$$

Consider this force expressed in terms of aerodynamic coefficients L_θ and $L_{\dot{\theta}}$ such that

$$L_{circ}(\theta, \dot{\theta}) = L_\theta \theta + L_{\dot{\theta}} \dot{\theta} \tag{41}$$

The complex valued representation employed in the legacy flutter tool would consider the following aerodynamic coefficients:

$$L_\theta = 2\pi\rho U_\infty^2 b C(k) \tag{42}$$

$$L_{\dot{\theta}} = 2\pi\rho U_\infty C(k) b^2 \left(\frac{1}{2} - a\right) \tag{43}$$

However, using the assumed oscillatory motion in Eqs. 37 through 39 and Eq. 36 one may arrive at real valued coefficients such that

$$L_\theta = 2\pi\rho U_\infty^2 b \left[F(k) - G(k) b \left(\frac{1}{2} - a\right) \omega \right] \tag{44}$$

$$L_{\dot{\theta}} = 2\pi\rho U_\infty b \left[G(k) U_\infty + F(k) b \left(\frac{1}{2} - a\right) \right] \tag{45}$$

This approach is detailed by Wright and Cooper (Ref. 5) and can be employed in a finite element representation. The resulting system is a completely real valued representation, that is more amenable to conventional structural dynamics analysis. That is, the system retains complex conjugate eigenvalue pairs and conventional frequency and damping extraction routines can be employed to extract physically meaningful frequency and damping values for the aeroelastic system.

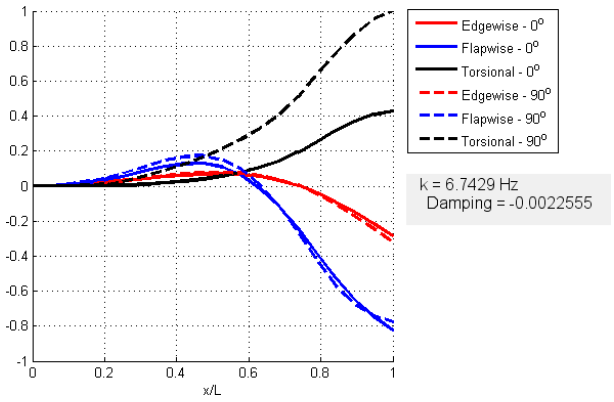

Fig. 8. WindPACT 1.5MW flutter mode shape predicted using real valued BLAST

REAL VALUED AEROELASTIC REPRESENTATION IN BLAST

The aforementioned alternative real valued aeroelastic representation was implemented into the BLAST analysis framework. As mentioned before, this representation has the benefit of resulting in a system with real valued coefficients, complex conjugate eigenvalue pairs, and is compatible with a well understood method for extraction of frequency and damping characteristics from eigenvalues of the system.

The Wind PACT 1.5MW blade was analyzed using a real valued aeroelastic representation in BLAST, and the frequency and damping versus rotor speed trends are shown in Figure 7. As expected, the eigenvalues of this system occur in complex conjugate pairs. Furthermore, "hard" flutter onset is observed at a rotor speed of 40.6 RPM (a 4% difference relative to the 42.3 RPM "hard" flutter mode observed for the BLAST analysis with a complex valued representation). The mode shape associated with this flutter mode is shown in Figure 8. The shape is a bit different than that predicted from the complex valued aeroelastic representation(Figure 5), but is indicative of a flutter mode with a 2nd flapwise component, and a first torsional component.

The SNL100-00 blade was also analyzed using the real valued implementation in BLAST. The frequency and damping vs. rotor speed trends for this analysis are shown in Figure 9. Hard flutter onset is observed at 13.05 RPM, and the mode shape associated with this flutter mode is shown in Figure 10. The mode shape is indicative of a flutter mode with 2nd flapwise components and 1st torsional components. This flutter rotor speed is between the softer 9.68 RPM and harder 14.40 RPM flutter speeds predicted by the complex valued aeroelastic representation in BLAST. These potential flutter speeds have a 26% and 10% difference respectively to the 13.05 RPM prediction from the real valued representation. Thus, for the larger blade, the differences between the two representations become more significant. Perhaps more noteworthy is that the real aeroelastic representation predicts a flutter margin (1.75) that is much higher than initial estimates for this blade.

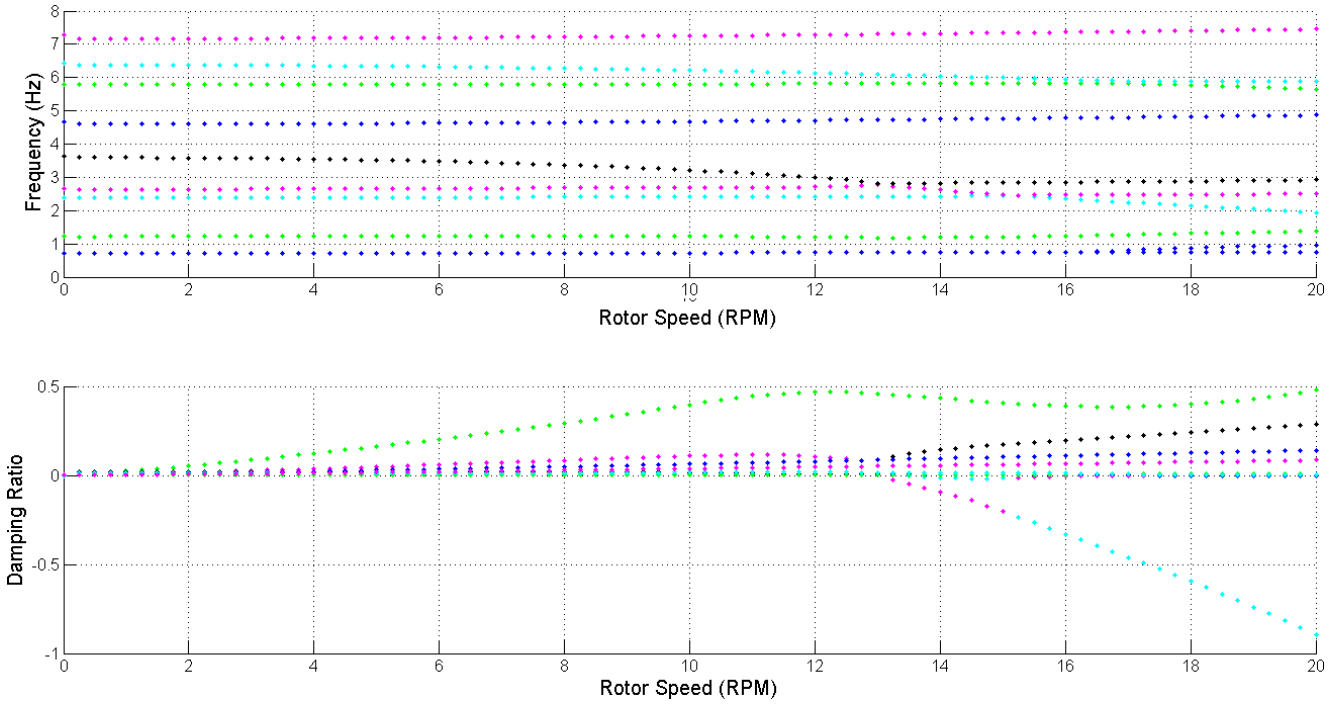

Fig. 9. Frequency and damping ratio vs. rotor speed real valued BLAST predictions for SNL100 blade

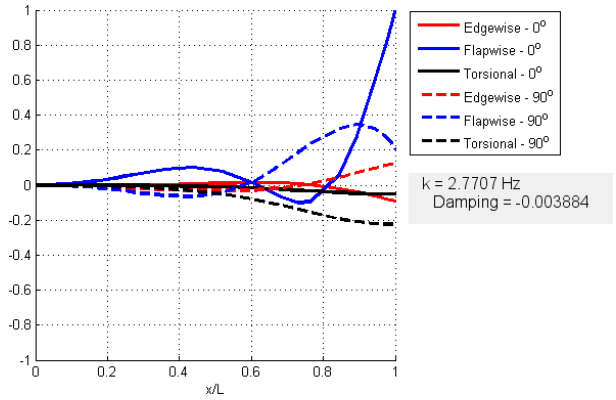

Fig. 10. SNL100-00 flutter mode shape predicted using real valued BLAST

CONCLUSIONS AND FUTURE WORK

This paper has presented an overview of the newly developed BLAST design tool for examining aeroleastic stability of wind turbine blade designs. The features of the tool and enhancements relative to a NASTRAN based legacy flutter tool were also discussed. The custom finite element framework in BLAST is written in the MATLAB programming environment. This makes for a flexible and extensible implementation that is extremely portable and integrates with existing blade design tools such as SNL NuMAD. BLAST was applied to a utility scale 1.5MW blade as well as the SNL100-00 100 meter all glass blade design. In the process, some potential issues with the modeling approach were identified which may be a more significant concern for larger blade types such as the SNL100 series. Indeed, consideration of a simple, single degree of freedom system showed that the complex valued representation employed in BLAST and the legacy flutter tool in general do not have complex conjugate pair eigenvalues and the extraction of frequency and damping from these eigenvalues using methods developed for conventional real valued systems should be reassessed.

Future work should further investigate the use of a complex valued aeroelastic representation in BLAST and ensure that frequency and damping information in a being extracted in a manner that is consistent with complex representations. Alternatively, a real valued aeroelastic representation may be employed. This approach would allow for much of the existing analysis methods developed for conventional real valued structural dynamic systems to be employed. Finally, initial flutter predictions for the SNL100 series using the legacy flutter tool showed an extremely narrow flutter margin for the very large blade. Revised analysis of this blade using BLAST show a larger flutter margin that may indicate flutter is not as crucial a concern in these blades. Nevertheless, future work should ensure current design tools are capable of adequately predicting flutter in very large wind turbine blades. Differences in BLAST predictions compared to those of the legacy flutter tool are mainly due to the higher fidelity geometric representation and automated procedures that remove the analyst from tedious iterative procedures. Such manual iterative procedures may limit the scope of flutter investigations, and the newly developed BLAST allows for a more thorough aeroelastic stability prediction. As a better understanding of the impact of aeroelastic representation is realized the sensitivity of large blade designs to flutter should be reevaluated, and modeling approaches in design tool should be updated accordingly.

REFERENCES

[1]Lobitz, D., "Aeroelastic Stability Predictions for a MW-sized Blade," *Wind Energy*, Vol. 7, 2004, pp. 211–224.

[2]Resor, B., Owens, B., and Griffith, D., "Aeroelastic Instability of Very Large Wind Turbine Blades," European Wind Energy Association Conference and Exhibition, April 2012.

[3]Bisplinghoff, R., Holt, A., and Halfman, R., *Aeroelasticity*, Dover, New York, New York, 1996.

[4]Hodges, D. and Pierce, G., *Introduction to Structural Dynamics and Aeroelasticity*, Cambridge, New York, New York, second edition, 2011.

[5]Wright, J. and Cooper, J., *Introduction to Aircraft Aeroelasticity and Loads*, Wiley, Hoboken, New Jersey, first edition, 2008.

[6]Meirovitch, L., *Computational Methods in Structural Dynamics*, Stijhoff & Noordhoff International Publishers, 1980.

[7]NASA, *The NASTRAN User's Manual*, June 1986.

[8]Douglas, F., *The NASTRAN Programmer's Manual*, NASA, January 1980.

[9]Hansen, M., "Aeroelastic Instability Problems for Wind Turbines," *Wind Energy*, Vol. 10, 2007, pp. 551–577.

[10]Berg, J. and Resor, B., "Numerical Manufacturing and Desing Tool (NuMAD v2.0) for Wind Turbine Blades: User's Guide," Technical Report SAND2012-7028, Sandia National Laboraotires, Albuquerque, New Mexico, 2012.

[11]Malcolm, D. and Laird, D., "Extraction of Equivalent Beam Properties from Blade Models," *Wind Energy*, Vol. 10, 2007.

[12]Bir, G., *User's Guide to PreComp*, National Renewable Energy Laboratory, Golden, Colorado, 2005.

[13]Cesnik, C. and Hodges, D., "VABS: A New Concept for Composite Rotor Blade Cross-Sectional Modeling," *Journal of the American Helicopter Society*, Vol. 42, 1997, pp. 27–38.

[14]Schaub, H. and Junkins, J., *Analytical Mechanics of Space Systems*, American Institute of Aeronautics and Astronautics, Reston, Virginia, 2003.

[15]Reddy, J., *An Introduction to the Finite Element Method*, McGraw Hill, New York, New York, third edition, 2005.

[16]Griffin, D., "WindPACT Turbine Rotor Design Scaling Studies Technical Area 1 - Composite Blades for 80-120 Meter Rotor," Technical report, National Renewable Energy Laboratory, Golden, Colorado, 2001.

[17]Griffith, D. and Ashwill, T., "The Sandia 100-meter All-glass Baseline Wind Turbine Blade: SNL100-00," Technical Report SAND2011-3779, Sandia National Laboratories, Albuquerque, New Mexico, 2001.